

Comparing Alternative Flood Mitigation Strategies For Non-Engineered Masonry Structures Using Demand and Capacity Factored Design

Stefano Carozza

Ph. D. Student, Dept. of Struct. for Engineering and Architecture, University of Naples Federico II

Fatemeh Jalayer

Associate Professor, Dept. of Struct. for Eng. and Architecture, University of Naples Federico II

Raffaele De Risi

Ph. D., Dept. of Struct. for Engineering and Architecture, University of Naples Federico II

Gaetano Manfredi

Professor, Dept. of Struct. for Engineering and Architecture, University of Naples Federico II

Elinorata Mbuya

Ph.D. Student, Institute of Human Settlements Studies (IHSS), Ardhi University, Tanzania

ABSTRACT: A closed-form performance-based safety-checking format known as the Demand and Capacity Factored Design (DCFD) is used in order to compare alternative flood mitigation strategies for non-engineered masonry structures. The structural fragility is evaluated by adopting an efficient and simulation-based method yielding the so-called “robust” fragility curve and an associated plus/minus one-standard deviation interval. The structural performance is measured by the (critical) demand to capacity ratio for the weakest element of the weakest wall within the structure, subjected to a combination of hydro-static, hydro-dynamic and accidental debris impact loads. Analogous to the incremental dynamic analysis method proposed for seismic demand assessment, an incremental hydraulic analysis has been implemented in order to monitor the structural performance as a function of increasing water height. In particular, the incremental hydraulic analysis has been employed in order to calculate the critical water height corresponding to a demand to capacity ratio of unity. This procedure has been illustrated for comparative evaluation of the factored demand and factored capacity for the case-study building hypothetically subjected to various flood mitigation strategies. The case-study application focuses on a one-story cement-brick non-engineered building located in Dar es Salaam, Tanzania.

A large percentage of the residential houses in Africa are classified as informal non-engineered buildings. They are characterized by their generally low quality of construction and are often constructed without formal criteria. Buildings belonging to this category are often constructed with substandard construction practice and their material mechanical properties are not well-documented. Furthermore, these structures are often located in flood-prone areas and their resistance capacity are inadequate.

Various research efforts have been focused

on different aspects of flooding risk assessment, such as loss of life (Jonkman et al. 2008; Tapsell et al. 2002), economic losses (Pistrika 2009; Pistrika and Tsakiris 2007), and damage to buildings (Bouchard 2007; Schwarz and Maiwald 2008; Smith 1994). Many studies have been performed in order to assess the vulnerability of a building in terms of damage state probability for the impact of debris flow (Haugen and Kaynia 2008), for riverine and coastal floods (Nadal et al. 2009), and for flood-prone informal settlements (De Risi et al. 2013a).

In this work, a probability-based safety checking format known as the Demand and Capacity Factored Design (DCFD) (Cornell et al. 2002) is implemented in order to compare alternative upgrading solutions against flooding.

As demonstrated in Jalayer et al. (Under review), the incremental analysis philosophy introduced by Vamvatsikos and Cornell (2002) has been adapted for flood vulnerability assessment. As the case study, a non-engineered one-storey building made of cement bricks with cement-based mortar is analyzed and the DCFD safety-checking format is applied in order to compare different upgrading solutions for this building. The alternative mitigation strategies proposed are all relatively low-cost and are based on measures that are already implemented by the inhabitants of the zone.

1. METHODOLOGY

1.1. Limit states and the source of uncertainty

The efficacy of different mitigation strategies is compared herein for the collapse limit state (CO). The CO limit state threshold is defined as the critical water height corresponding to loss of bearing capacity of the structure (e.g. loss of support of the roof, collapse of walls, loss of load bearing capacity due to elongated contact with water or deterioration). The structural collapse limit state is defined in terms of a structural performance variable denoted as Y . Following a weakest link formulation (Ditlevsen and Madsen 1996), Y is defined as the systemic demand to capacity ratio and is equal to unity at the onset of the limit state. Given the potentially fragile nature of collapse and the possible lack of box behavior, the weakest link formulation seems to be suitable for describing the systemic behavior of non-engineered masonry structures.

Inspired from the works of Jalayer and Cornell (2003) and Jalayer et al. (2007) which also adopt an IM-based safety checking, the water height is used as an interface variable (a.k.a. intensity measure IM) between flood fragility and hazard. Accordingly, the onset of limit state is marked as the critical water height correspond-

ing to the collapse limit state (denoted as $h^{Y=1}$).

The flooding fragility is defined as the probability of exceeding the limit state conditioned on the flooding height h . It can also be described as the cumulative distribution function for the performance variable $h^{Y=1}$:

$$P(LS | h) = P(Y > 1 | h) = P(h^{Y=1}(\boldsymbol{\theta}) < h) \quad (1)$$

where $\boldsymbol{\theta}$ is the vector of the uncertain parameters. Generally, the uncertainties can be classified in two main categories: (a) the uncertainties in the characterization of the structural modelling parameters; (b) the uncertainties in loading.

1.2. Bayesian fragility assessment procedure using Monte Carlo simulations

The structural fragility is evaluated employing an efficient Bayesian simulation-based method that leads to a “robust” fragility curve and an associated plus/minus logarithmic standard deviation interval (Jalayer et al. 2013) based on a Log Normal fragility model. Let \mathbf{D} denote the vector of critical flooding height values corresponding to $Y=1$ (obtained through the incremental hydraulic analysis explained in next section), calculated for a limited number of realizations of the vector $\boldsymbol{\theta}$. The Log Normal analytic fragility function can be described as:

$$F(LS | h, \boldsymbol{\chi}) = P(h^{Y=1} \leq h | \eta, \beta) = \Phi\left(\frac{\ln(h/\eta)}{\beta}\right) \quad (2)$$

where the parameters $\boldsymbol{\chi} = [\log \eta, \beta]$ represent the (log of) median and the logarithmic standard deviation of the critical flood water height corresponding to the exceedance of limit state and denoted as $h^{Y=1}$. Conditioned on \mathbf{D} , the posterior joint probability distribution for $\boldsymbol{\chi}$ based on a non-informative prior distribution can be expressed as:

$$p(\boldsymbol{\chi} | \mathbf{D}) = p(\log \eta | \beta, \mathbf{D}) \cdot p(\beta | \mathbf{D}) \quad (3)$$

where $p(\beta | \mathbf{D})$ is the posterior marginal distribution of β and $p(\log \eta | \beta, \mathbf{D})$ is the posterior conditional distribution of $\log \eta$ given β . The marginal PDF for β can be expressed as a derived $\boldsymbol{\chi}$ distribution:

$$p(\beta | \mathbf{D}) = \left[\frac{1}{2} \cdot \Gamma \cdot \left(\frac{n}{2} \right) \right]^{-1} \cdot \left(\frac{\nu \cdot s^2}{2} \right)^{\frac{n}{2}} \cdot \beta^{-(n+1)} \cdot e^{-\frac{\nu \cdot s^2}{2 \cdot \beta^2}} \quad (4)$$

The posterior conditional distribution of η can be calculated as a multi-variate Normal distribution:

$$p(\log \eta | \beta, \mathbf{D}) = \sqrt{\frac{N}{2 \cdot \pi \cdot \beta^2}} \cdot e^{-\frac{N(\ln \eta - \overline{\ln h^{Y=1}})^2}{2 \cdot \beta^2}} \quad (5)$$

here $\nu=N-1$; $\overline{\ln h^{Y=1}}$ and s^2 are the (logarithmic) sample average and sample variance of the set of structural performance variable values $h^{Y=1}$ for limit state LS , respectively. Finally, the *robust fragility* can be calculated by integrating over the joint (posterior) probability distribution for the parameters of the Log-Normal fragility model conditioned on the set of data values obtained in the form of $D = \{D_i = h_i^{Y=1}\}$:

$$\begin{aligned} P(LS | h, \mathbf{D}) &= E_{\chi}[F(LS | h, \mathbf{D}, \chi)] = \\ &= \int_{\Omega(\chi)} \Phi\left(\frac{\ln(h/\eta)}{\beta}\right) \cdot p(\chi | \mathbf{D}) \cdot d\chi \end{aligned} \quad (6)$$

where $E_{\chi}[\cdot]$ is the expected value operator over the vector of parameters $\chi = [\log \eta, \beta]$ and Ω is the domain of vector χ . The variance σ^2 in fragility estimation can be calculated as:

$$\begin{aligned} \sigma_{\chi}^2 F &= E_{\chi}[F(LS | h, \mathbf{D}, \chi) - P(LS | h, \mathbf{D})]^2 = \\ &= \int_{\Omega(\chi)} \left[\Phi\left(\frac{\ln(h/\eta)}{\beta}\right) - P(LS | h, \mathbf{D})\right]^2 \cdot p(\chi | \mathbf{D}) \cdot d\chi \end{aligned} \quad (7)$$

where $P(LS|h, \mathbf{D})$ is calculated from Eq. (6).

Using Monte Carlo Simulation, it is possible to evaluate the robust fragility curve and its plus/minus one standard deviation confidence interval approximating Eq. (6) and Eq. (7) in the following manner:

$$P(LS | h, \mathbf{D}) \approx \tilde{R} = \frac{\sum_{i=1}^{n_{sim}} \Phi\left(\frac{\ln(h/\eta_i)}{\beta_i}\right)}{n_{sim}} \quad (8)$$

and

$$\sigma_{\chi}^2 F \approx \frac{\sum_{j=1}^{n_{sim}} \left[\Phi\left(\frac{\ln(h/\eta_j)}{\beta_j}\right) - \tilde{R}\right]^2}{n_{sim}} \quad (9)$$

where n_{sim} is the number of simulations. In above equations, η_i and β_i correspond to the i^{th} realization of the vector of fragility parameters χ_i . The

vector χ_i is simulated based on its probability density function $p(\chi|\mathbf{D})$ in Eq. (3). This is achieved by first sampling β_i from its (posterior) marginal probability distribution $p(\beta|\mathbf{D})$ in Eq. (4). In the next step, conditioning on β_i , η_i is sampled from the conditional (posterior) distribution $p(\log \eta|\beta_i, \mathbf{D})$ in Eq. (5). It should be noted that n_{sim} can assume very large values with no computational problem as the estimators shown in Eq. (8) and Eq. (9) and the probability distributions in Eq. (4) and Eq. (5) are all expressed in a closed and analytic form.

1.3. Incremental Hydraulic Analysis (IHA) in a performance based-based safety-checking framework

The incremental hydraulic analysis (IHA) is a procedure for evaluating the critical demand to capacity ratio Y with increasing values of flooding height for given realizations of uncertain parameters θ . The resulting $Y-h$ data points (evaluated at each increasing value of flooding height h) can be connected in order to form the IHA curves as shown in Figure 1.

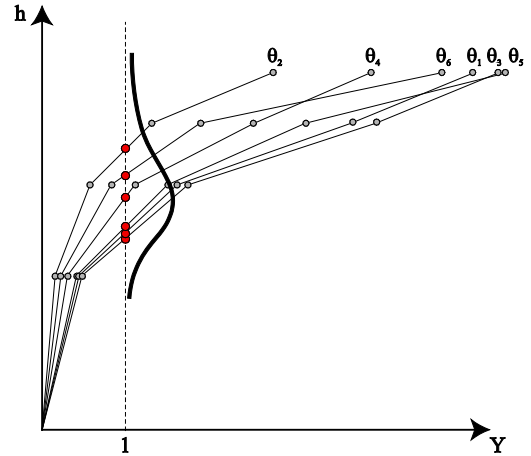


Figure 1: Typical incremental hydraulic analysis curves.

As shown in Figure 1, IHA curves can be used to find the critical water height corresponding to reaching of a prescribed limit state interpolating the curves in correspondence of $Y=1$.

Denoting the mean annual frequency of exceeding a prescribed limit state as λ_{LS} and an acceptable level of risk as λ_0 , a performance-based safety-checking expression can be written as:

$$\lambda_{LS} = \int_{\Omega_h} P(LS|h, \mathbf{D}) |d\lambda(h)| \leq \lambda_o \quad (10)$$

where $P(LS|h, \mathbf{D})$ is the robust flooding fragility curve and $\lambda(h)$ is the flooding hazard expressed in terms of mean annual frequency of exceeding a certain flood height h .

Assuming that (Cornell et al. 2002; Jalayer and Cornell 2004): (a) the fragility $P(LS|h, \mathbf{D})$ can be expressed as a Log Normal distribution function with median $\eta_{h(Y=1)}$ and logarithmic standard deviation $\beta_{h(Y=1)}$; (b) the flooding hazard curve can be approximated by a power-low relation as function of the flooding height $k_o \cdot h^{-k}$, λ_{LS} in Eq. (10) can be reduced to the closed-form :

$$\lambda_{LS} = k_o \cdot (\eta_{h^{Y=1}})^{-k} \cdot \exp\left(\frac{1}{2} k^2 \cdot \beta_{h^{Y=1}}^2\right) \leq \lambda_o \quad (11)$$

Eq. (11) can be re-organized as follow:

$$\left(\frac{\lambda_o}{k_o}\right)^{\frac{-1}{k}} \leq \eta_{h^{Y=1}} \cdot \exp\left(-\frac{1}{2} k \cdot \beta_{h^{Y=1}}^2\right) \quad (12)$$

The inequality written in Eq. (12) can be represented in a generic format:

$$h(T_R) = \left(\frac{\lambda_o}{k_o}\right)^{\frac{-1}{k}} \leq FC \quad (13)$$

where $h(T_R)$ is the flooding height corresponding to the flooding return period $T_R=1/\lambda_o$ from the flood hazard curve or simply “flood demand”; FC is the factored critical flooding height or simply “factored capacity”:

$$FC = \eta_{h^{Y=1}} \cdot \exp\left(-\frac{1}{2} k \cdot \beta_{h^{Y=1}}^2\right) \quad (14)$$

After taking into account the epistemic uncertainties, Eq. (14) evolves into the following equation (Cornell et al. 2002):

$$FC_U = \eta_{h^{Y=1}} \cdot \exp\left(-\frac{1}{2} k \cdot \beta_{h^{Y=1}}^2\right) \cdot \exp\left(-\frac{1}{2} k \cdot \beta_U^2\right) \quad (15)$$

where β_U represents the epistemic uncertainties in the estimation of the median flooding height. It turns out that $\beta_{h(Y=1)}$ and β_U can both be evaluated from the robust fragility curve and its plus/minus one standard deviation confidence interval:

$$\beta_{h^{Y=1}} = \frac{1}{2} \cdot \ln \frac{h_{84^{th}}}{h_{16^{th}}} \quad ; \quad \beta_U = \frac{1}{2} \cdot \ln \frac{h^+}{h^-} \quad (16)$$

where $h_{84^{th}}$ and $h_{16^{th}}$ are the 84th and 16th percentiles of the critical flooding height; h^+ and h^- are the median critical water height calculated from the robust fragility plus and minus one standard deviation curves, respectively. Figure 2 shows a schematic representation of the various elements to be considered in the DCFD safety-checking format. The red curve is representative of the flooding hazard, while the blue curves represent the robust fragility (solid line) and its plus/minus one standard deviation fragility curves (dashed line).

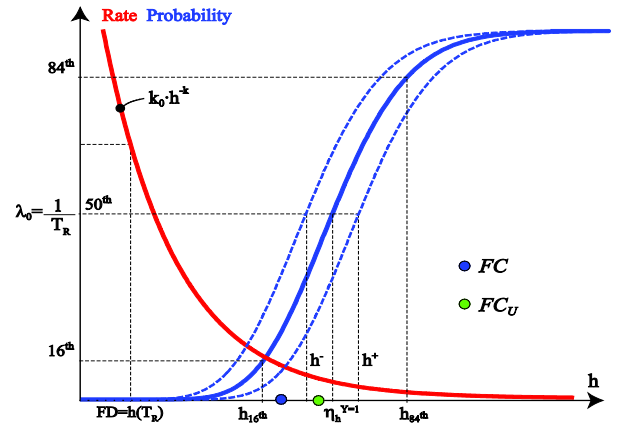


Figure 2: A schematic diagram of the DCFD safety-checking format.

1.4. Flood actions

In this work, the structural damage induced by flooding is assumed to be due to the sum of hydrostatic and hydrodynamic pressure profile, at a given height from the ground level, and the accidental action induced by the impact of waterborne debris (Kelman and Spence 2004). The hydrostatic pressure $p_{hs}(z)$ is governed by Stevin’s law, and can be calculated as described in Eq. (17).

$$p_{hs}(z) = \gamma_w \cdot (h - z) \quad (17)$$

The hydrodynamic action considered in this work is only due to velocity of flow and ignores the action due to transient water level (Roos et al. 2003). The hydrodynamic pressure at height z from ground can be calculated as:

$$p_{hd}(z) = C_d \cdot \rho_w \cdot v^2(z) \quad (18)$$

where C_d is the drag coefficient (assumed between 1.2 and 2.0 (Roos et al. 2003)); ρ_w is the mass density of water ($\rho_w = \gamma_w/g$, with g gravity acceleration); $v(z)$ is the flow velocity at height z assumed as a parabolic profile (Eq. (19)).

$$\frac{v(z)}{v_{\max}} = -\left(\frac{z}{h}\right)^2 + 2 \cdot \left(\frac{z}{h}\right) \quad (19)$$

The relation between the maximum flooding velocity and maximum flooding height at any given point within the zone of interest can be approximated with a power-law relation in the form $v_{\max} = a \cdot h_{\max}^b$ (De Risi et al. 2013a; De Risi et al. 2013b). This power-law fit helps in transforming an otherwise vector-based risk assessment using $\mathbf{H} = [h_{\max}, v_{\max}]$ as the hazard/fragility interface variable to a scalar risk assessment problem using only h_{\max} as the interface variable. Once the velocity profile is known, it is possible to calculate the (accidental) debris impact force F_{DI} adopting an impulse-momentum formulation (FEMA 1995):

$$F_{DI} = \frac{W_D \cdot v_D}{g \cdot t} \quad (20)$$

where W_D is the debris weight; v_D is the debris velocity; g is the gravity acceleration; and t is impact duration. Within the simulation procedure, the debris mass, the impact duration and the horizontal position of the point of impact along the wall are going to be randomized.

2. CASE STUDY: A NON-ENGINEERED CEMENT BLOCKS BUILDING

The case study building is a masonry cement blocks structure, which is a typical residential construction located in the Suna neighborhood in Dar Es Salaam (Carozza et al. 2013). Based on a detailed survey conducted by the Institute of Human Settlements Studies (IHSS, Ardhi University), the walls of the building are not protected with a waterproof layer and have a thickness equal to the thickness of cement block (125mm) plus the plaster thickness of 10-20mm.

2.1. Structural model and characterization of the uncertainties

The structural model employed in this work con-

sists of a two-dimensional elastic finite shell element panel with void openings analyzed in the open-source software OpenSees (McKenna et al. 2006). Based on the field survey, the roof consists of a very thin and deformable metal sheet and the vertical connections between the walls do not seem sufficient for guaranteeing the box action. As a result, the structure is modeled as an ensemble of individual 2D wall panels hinged along the vertical side and fixed at the bottom. Figure 3 depicts the geometrical model. In order to take into account the considerable amount of uncertainties in mechanical characterization of structure (both due to degradation and also due to lack of laboratory tests), the probability distributions reported in Table 1 were considered for the mechanical properties.

Table 1: Mechanical prop. for case study building

Mech. properties	Distr. type	Min	Max
γ (kN/m ³) specific weight	Uniform	14.0	18.0
f_m (MPa) compress. strength	Uniform	1.0	3.0
τ (MPa) shear strength	Uniform	0.03	0.1
f_l (MPa) flexural strength	Uniform	0.2	1.5
E (MPa) elastic modulus	Uniform	1200	1200

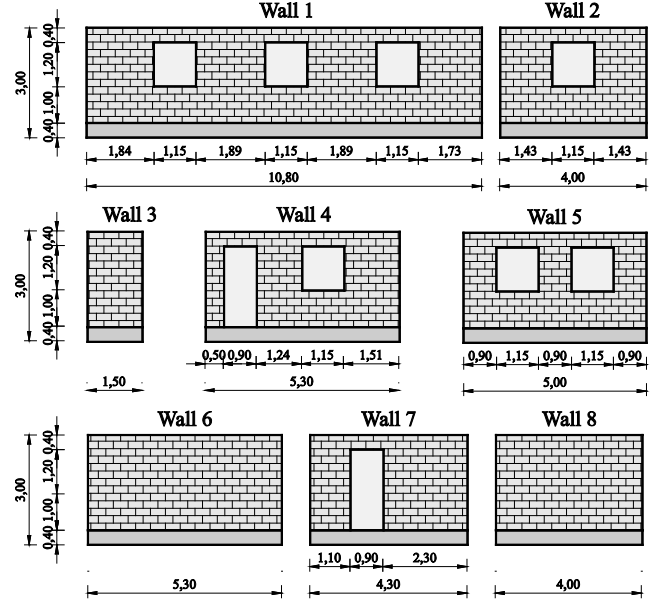


Figure 3: 2D walls model in OpenSees (meters)

In addition, in order to take into account the visual signs of degradation in the case study building, a reduction coefficient of 0.75 has been applied to all mechanical properties (De Risi et al. 2012). According to the survey, the doors and windows are not sufficiently water-proof and the

hydrostatic pressure is applied only until water can enter inside the building. The uncertainty in debris weight and duration impact is modeled as reported in Table 2. The a and b coefficients for the velocity profile ($v_{max}=a \cdot h_{max}^b$) are equal to 0.093 and 1.15, respectively (based on the calculated inundation maps, see De Risi et al. 2013).

Table 2: Loading parameters

Loading parameter	Distr. type	Min	Max
Debris mass (kg)	Uniform	200	500
Impact duration (s)	Uniform	0.5	1.5

The horizontal position in which the debris force is applied on the wall is randomized for each wall; whereas, the vertical position depends on flooding height (assuming floating debris).

2.2. Incremental Hydraulic Analysis (IHA)

The performance variable Y is calculated as the largest demand to capacity ratio throughout all the walls within the structure. In each wall, safety checking is performed in different critical sections (i.e. horizontal base section, vertical side sections, horizontal and vertical middle sections, and sections on the edge of the openings) so that all the possible failure mechanisms are taken into account. For each of these sections, an iterative procedure is performed in order to identify the subsection in which the demand to capacity ratio is the largest.

The flexural and shear stress capacities are evaluated as follow (De Risi et al. 2013b).

$$M_{Rd,H} = \frac{N \cdot t_w}{2} \cdot \left(1 - \frac{N}{0.85 \cdot f_m \cdot A_{section}} \right) \quad (21)$$

$$V_{Rd} = A_{section} \cdot \tau_0 \quad M_{Rd,V} = \frac{f_{fl} \cdot H_{section} \cdot t_w^2}{6} \quad (22)$$

where $M_{Rd,H}$ is the flexural strength of a horizontal section; $M_{Rd,V}$ is the flexural strength of a vertical section; V_{Rd} is the shear strength; $A_{section}$ is the area of the section/sub-section; $H_{section}$ is the height of the section/sub-section, N is the axial force acting on the section/sub-section and t_w is the thickness of the wall. For a given realization of vector Θ , the critical demand to capacity ratio Y is calculated as the largest demand to capacity ratio considering both the shear stress and the out-of-plane bending moment. In other words, Y

is equal to:

$$Y = (D/C)_{Weakest-link} \quad (23)$$

Figure 4 reports the IHA curves for the simulation realizations performed for the case study building. It can be seen that for the considered structure, the critical flood height is not particularly sensitive to the considered uncertainties in loading and mechanical material properties (note that the wall thickness is deterministic).

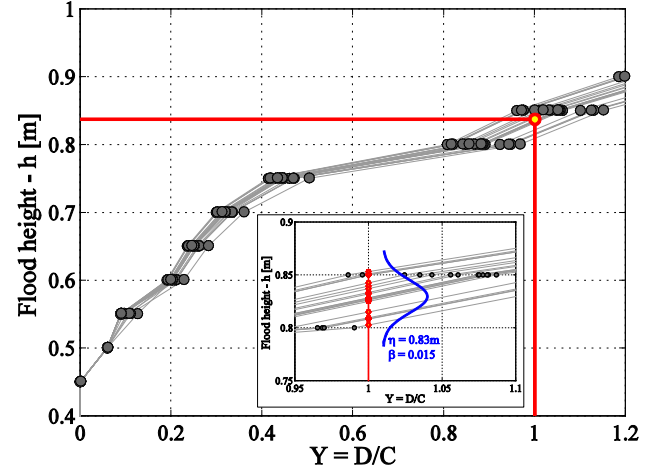


Figure 4: Incremental Hydraulic Analysis curves for various realization of the vector θ .

2.3. Performance-based safety-checking for different flood mitigation strategies

In order to compare alternative mitigation strategies for the case study building, DCFD format is used and the results are depicted in Figure 5. The strategies taken into account are designed departing from the as-built configuration of the building (model D, purple) and are described below.

Increasing Platform Height. This strategy (model A, green) consists in increasing the level of platform from 40cm to 80cm. The pressure of the water on the walls (that depends on the water height) is substantially reduced so that this strategy leads to a significant reduction of the risk.

Upgrading vertical connection. In this case, (model B, orange) the corner details between the walls are improved using reinforcement or special placing of bricks in the wall corners (in the model, the boundary conditions change from hinged to clamped). It is worth noting that a good vertical connection may ensure the presence of box effect and a 3D model would be

much more suitable for representing the overall performance of the structure.

Filling door in Wall 4. This strategy (model C, dark blue) consists in filling the opening in Wall 4 in order to reduce the stress concentration in the small horizontal base section between the door and the side of the wall.

Reorganization of openings. This solution (model E, dark green) consists in the filling of the existing doors in walls 4 and 7 (that make the stress distribution in the walls more irregular) and creating a new door replacing the central window of the Wall 1.

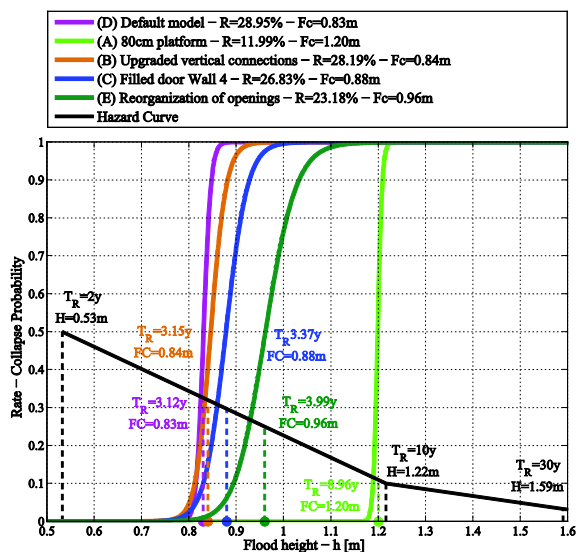


Figure 5: DCFD for different mitigation strategies

In Figure 5 the different mitigation strategies proposed for the case study are compared in terms of: (a) fragility curves; (b) factored capacity FC ; (c) return period capacity T_R ; (d) risk value (reported in the legend). The figure demonstrates that DCFD format is a clear and quantitative instrument for comparing different solutions applied in order to reduce flooding vulnerability. In the specific case, the best mitigation strategy (among those proposed) is to increase the height of platform. This scope may be reached by raising the ground floor thickness inside the building by 40cm and, as it can be observed in the figure, leads to a reduction in risk from 29% to 12%.

3. CONCLUSIONS

DCFD is a performance- and probability-based format used in this work for flood resistance up-

grade decision-making for non-engineered masonry buildings. In the case study, different viable mitigation strategies are proposed in order to reduce the flooding vulnerability. The proposed approaches are all relatively low-cost and some of them are already implemented by the inhabitants of the zone as climate adaptation strategies. In particular, a few viable mitigation strategies are compared in terms of their return period capacities and risk. For the particular typology of building considered, increasing the platform height and the reorganization of the openings are identified as the more efficient strategies. The first one reduces significantly the stress on the walls since it reduces the height of the wall exposed to flooding load. The second one promotes a more balanced stress distribution in the walls around the openings.

4. ACKNOWLEDGEMENTS

This work was supported in part by the European Commission's seventh framework program Climate Change and Urban Vulnerability in Africa (CLUVA), FP7-ENV-2010, Grant No. 265137 and the National Operative Program Project METROPOLIS 2014-16.

5. REFERENCES

- Bouchard, B. (2007). "Improving flood risk management in informal settlements of Cape Town."
- Carozza, S., De Risi, R., and Jalayer, F. (2013). "D2.5 - Guideline to Decreasing Physical Vulnerability in the Three Considered Cities." *CLUVA project - Climate Change and Urban Vulnerability in Africa*.
- Cornell, C. A., Jalayer, F., Hamburger, R. O., and Foutch, D. A. (2002). "Probabilistic basis for 2000 SAC Federal Emergency Management Agency steel moment frame guidelines." *Journal of Structural Engineering*, 128(4), 526-533.
- De Risi, R., Jalayer, F., De Paola, F., Iervolino, I., Giugni, M., Topa, M. E., Mbuya, E., Kyessi, A., Manfredi, G., and Gasparini, P. (2013a). "Flood risk assessment for informal settlements." *Natural Hazards*, 69(1), 1003-1032.

- De Risi, R., Jalayer, F., Iervolino, I., Kyessi, A., Mbuya, E., Yeshitela, K., and Yonas, N. (2012). "D2.4 - Guidelines for vulnerability assessment and reinforcement measures of adobe houses." *CLUVA project - Climate Change and Urban Vulnerability in Africa*.
- De Risi, R., Jalayer, F., Iervolino, I., Manfredi, G., and Carozza, S. (2013). "VISK: a GIS-compatible platform for micro-scale assessment of flooding risk in urban areas." *Proc., COMPDYN, 4th ECCOMAS Thematic conference on computational methods in structural dynamics and earthquake engineering. Kos Island, Greece*.
- Ditlevsen, O., and Madsen, H. O. (1996). *Structural reliability methods*, Citeseer.
- FEMA, F. E. M. A. (1995). *Report 259. Engineering principles and practices for retrofitting floodprone residential buildings*, Washington, D.C., USA.
- Haugen, E. D., and Kaynia, A. M. (2008). "Vulnerability of structures impacted by debris flow." *Landslides and Engineered Slopes: From the Past to the Future, Vols 1 and 2*, 381-387.
- Jalayer, F., Carozza, S., De Risi, R., Manfredi, G., and Mbuya, E. (Under review). "Performance-based flood safety-checking for non-engineered masonry structures." *Engineering Structures*.
- Jalayer, F., and Cornell, C. A. (2003). "A special application of non-linear dynamic analysis procedures in probability-based seismic assessments in the region of global dynamic instability." *Applications of Statistics and Probability in Civil Engineering, Vols 1 and 2*, 1493-1500.
- Jalayer, F., and Cornell, C. A. (2004). *A technical framework for probability-based demand and capacity factor design (DCFD) seismic formats*, Pacific Earthquake Engineering Research Center.
- Jalayer, F., De Risi, R., Elefante, L., and Manfredi, G. (2013). "Robust fragility assessment using Bayesian parameter estimation." *Vienna Congress on Recent Advances in Earthquake Engineering and Structural Dynamics 2013 (VEESD 2013)*, R. H. C. Adam, W. Lenhardt & C. Schranz, ed. Vienna, Austria.
- Jalayer, F., Franchin, P., and Pinto, P. E. (2007). "A scalar damage measure for seismic reliability analysis of RC frames." *Earthquake Engineering & Structural Dynamics*, 36(13), 2059-2079.
- Jonkman, S. N., Vrijling, J. K., and Vrouwenvelder, A. C. W. M. (2008). "Methods for the estimation of loss of life due to floods: a literature review and a proposal for a new method." *Natural Hazards*, 46, 353-389.
- Kelman, I., and Spence, R. (2004). "An overview of flood actions on buildings." *Engineering Geology*, 73(3), 297-309.
- McKenna, F., Fenves, G. L., and Scott, M. H. (2006). "OpenSees: Open system for earthquake engineering simulation." *Pacific Earthquake Engineering Center, University of California, Berkeley, CA*.
- Nadal, N. C., Zapata, R. E., Pagán, I., López, R., and Agudelo, J. (2009). "Building damage due to riverine and coastal floods." *Journal of Water Resources Planning and Management*, 136(3), 327-336.
- Pistrika, A. (2009). "Flood Damage Estimation based on Flood Simulation Scenarios and a GIS Platform." *EWRA 7th International Conference "Water Resources Conservancy and Risk Reduction Under Climatic Instability"* Limassol, Cyprus, 419-427.
- Pistrika, A., and Tsakiris, G. (2007). "Flood risk assessment: A methodological framework." *Water Resources Management: New Approaches and Technologies. European Water Resources Association, Chania, Crete-Greece*.
- Roos, W., Waarts, P., and Vrouwenvelder, A. (2003). "Damage to buildings." *Delft Cluster paper*.
- Schwarz, J., and Maiwald, H. (2008). "Damage and loss prediction model based on the vulnerability of building types." *4th International symposium of Flood Defence* Toronto, Canada.
- Smith, D. (1994). "Flood damage estimation- A review of urban stage-damage curves and loss functions." *Water S. A.*, 20(3), 231-238.
- Tapsell, S. M., Penning-Rowsell, E. C., Tunstall, S. M., and Wilson, T. L. (2002). "Vulnerability to flooding: health and social dimensions." *Philos T Roy Soc A*, 360(1796), 1511-1525.
- Vamvatsikos, D., and Cornell, C. A. (2002). "Incremental dynamic analysis." *Earthquake Engineering & Structural Dynamics*, 31(3), 491-514.